# Planar metallic nanoscale slit lenses for angle compensation

Lieven Verslegers,[a] Peter B. Catrysse,[b] Zongfu Yu, and Shanhui Fan[c]
*Department of Electrical Engineering, E. L. Ginzton Laboratory, Stanford University, Stanford, California 94305, USA*

(Received 27 April 2009; accepted 30 July 2009; published online 21 August 2009)

We demonstrate numerically, using a modified total-field/scattered-field formalism, that metallic lenses, based on arrays of nanoscale slits with varying widths in a planar metallic film, can be used to focus light and compensate for various angles of incidence. These structures could be used as integrated microlenses to improve the efficiency of pixels in solid-state image sensors. Our design guidelines simultaneously accomplish a prism and focusing action. Our results also indicate the importance of the aperture effect for such far-field focusing devices. © *2009 American Institute of Physics*. [DOI: 10.1063/1.3211875]

Plasmonics has emerged as a technology that enables the creation of a wide range of miniaturized and nanostructured photonic devices.[1–3] Nanopatterned optically thick metallic films were suggested as a plasmonic alternative for shape-based dielectric optical components such as refractive lenses, prisms, and beam splitters.[4–7] A planar lens based on a nanoscale slit array was recently demonstrated experimentally.[8] The use of metal provides the advantage of much higher index contrast over dielectric structures, resulting in a stronger focusing capability for lenses as well as a convenient planar geometry.

In this letter, we numerically demonstrate the use of nanopatterned films as lenses that compensate for various angles of incidence. Our work is motivated in part by the need to enhance the efficiency of off-axis pixels in solid-state image sensors. In complementary metal-oxide-semiconductor image sensors, microlenses are widely used to focus light incident on pixels onto their photodetector. Such lenses are usually fabricated using a combination of lithography and reflow techniques,[9] which typically results in a periodic array of identical lens structures. The problem with identical lens structures is illustrated in Fig. 1(a). For off-axis pixels, since light is coming in at an angle, the focal point is shifted away from immediately underneath the lens, resulting in reduced efficiency and increased crosstalk. The standard solution involves shifting the identical microlenses inwards.[10] There has been recent work aiming to address this issue using subwavelength dielectric features in several layers.[11] Here we show that a planar plasmonic structure can transform the incident wave front and achieve far-field focusing in the vertical dimension (propagation direction) without horizontal displacement of the focal spot [Fig. 1(b)].

Figure 2(a) shows a metallic structure, designed to compensate for a 20° angle. It consists of a gold film (450 nm thick) on top of an oxide. Within the film are slits ranging from 10 to 100 nm in width. The lens is less than 1.75 $\mu$m wide and designed to focus at a distance of 4 $\mu$m centered underneath the structure on a semiconductor photodetector that is 1.2 $\mu$m wide. (These parameters are chosen based on volume-produced, state-of-the-art solid-state image sensors at the time of submission.) All calculations and simulations are performed at a wavelength of 632.8 nm. The permittivities of gold and oxide at this wavelength are $\varepsilon_m=-10.77+0.79i$ and $\varepsilon_{ox}=2.13$.[12]

In order to realize simultaneous angle compensation and focusing, the basic idea is to carefully tailor the phase front with the device. This is achieved by controlling the width and the positions of the slits. A deep subwavelength slit always supports propagating transverse magnetic modes,[13] with the phase index of the mode increasing as the slit width decreases. Moreover, in our structure the nearby slits are in sufficiently close proximity to each other such that they couple. In the case of two slits coupled to each other, the symmetric mode that has the same phase in the two slits has a lower phase index when the spacing becomes smaller. Both of these effects can be used to tune the local phase front. Analytically, to take into account the effect of both individual slit as well as their coupling, we calculate the local phase front below each individual slit by considering a periodic metallic waveguide array made of such slits. For the symmetric mode in such an array, the dispersion relation is[14]

$$\cos(k_1a_1)\cos(k_2a_2)-\left(\frac{\varepsilon_m^2k_1^2+k_2^2}{2\varepsilon_mk_1k_2}\right)\sin(k_1a_1)\sin(k_2a_2)=1 \tag{1}$$

with $k_1=(k_0^2-\beta^2)^{1/2}$ and $k_2=(\varepsilon_mk_0^2-\beta^2)^{1/2}$, where $a_1$ is the slit width, $a_2$ is the metal thickness, $k_0$ is the free space wave vector and $\beta$ is the propagation constant of the mode. From the propagation constant and for a film with thickness $d$, we can calculate the phase delay introduced by a single pass through a slit as $\mathrm{Re}(\beta)d$. Strictly speaking, the use of the

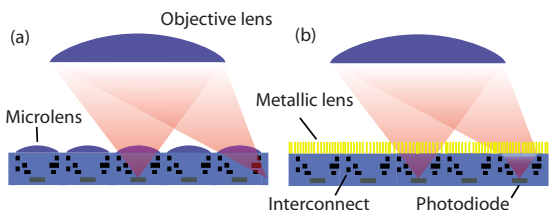


FIG. 1. (Color online) Motivation for focusing with angle compensation. (a) Schematic of conventional camera with short focal length objective lens (all microlenses are identical). Pixels on the periphery have reduced efficiency and more crosstalk. (b) Proposed architecture: optically thick planar metallic lenses compensate for the angle of incoming light.

[a]Electronic mail: lievenv@stanford.edu.
[b]Electronic mail: pcatryss@stanford.edu.
[c]Electronic mail: shanhui@stanford.edu.

 

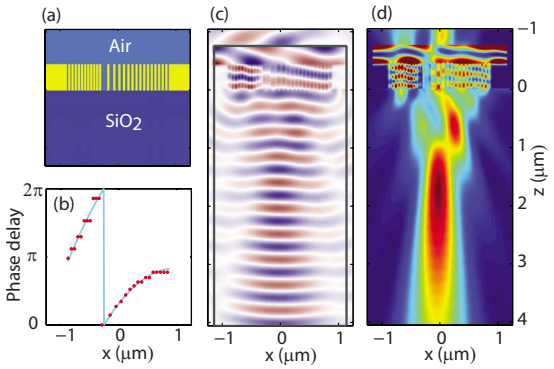


FIG. 2. (Color online) Planar metallic lens with 20° angle compensation. (a) Geometry of the lens made from gold film (yellow) with air slits (light blue) on silica substrate (dark blue). (b) The phase delay (up to an arbitrary constant) from Eq. (2) (blue line), mimicked by the array of slits (red dots) (slit sequence: 18, 2×16, 2×14, 3×12, 3×10, 100, 62, 46, 40, 34, 30, 28, 2×26, 2×24, and 5×22 nm spaced 40 nm apart). 2D FDFD magnetic field (c) and magnetic field intensity pattern (d). The gray lines indicate the boundary between total-field and scattered-field region. In order to show the features of the focus clearly, the intensity pattern is shown saturated near and inside the slits.

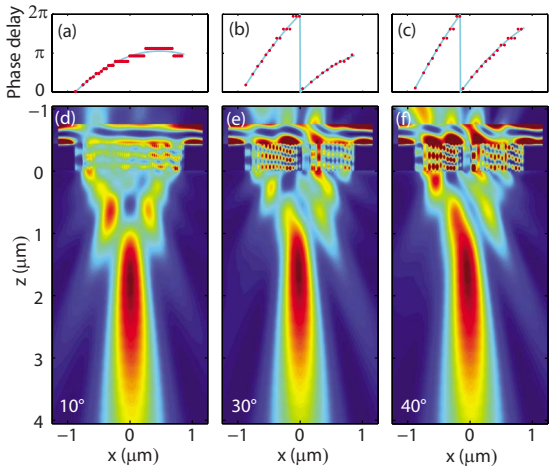


FIG. 3. (Color online) Planar metallic lenses compensating for different angles. The phase delay required (blue line) for (a) 10° (slit sequence: 100, 44, 34, 28, 26, 2×22, 20, 2×18, 3×16, 7×14, 8×12, 15×10, and 5×12 nm), (b) 30° (slit sequence: 72, 38, 28, 24, 20, 18, 16, 2×14, 3×12, 3×10, 100, 58, 44, 36, 32, 28, 26, 2×24, 22, and 20 nm), and (c) 40° (slit sequence: 94, 36, 26, 22, 18, 16, 2×14, 2×12, 2×10, 100, 44, 34, 28, 24, 22, 20, 18, 2×16, 3×14, and 2×12 nm) angle compensation and focusing, and as mimicked by a slit array (red dots). FDFD simulated focusing patterns [(d)–(f)].

symmetric mode dispersion relation is reasonable only when the angle of incidence is small (and, consequently, the phase does not differ much between neighboring deep-subwavelength slits). Nevertheless, our simulations indicate that this assumption works well for all the angles we considered here. Our simulations also indicate that this approach gives better prediction of the focusing behavior, when compared to the dispersion relation of an isolated slit that was used in previous work.[5,6,8]

For an oblique angle of incidence $\theta$, the phase of the incident plane wave is known exactly and can be compensated for, in order to achieve focusing directly beneath the plasmonic nanoslit lens structure. The required phase delay, as a function of position $x$ (with $x=0$ at the center of the lens) is [blue line in Fig. 2(b)]

$$\phi(x) = \frac{2\pi x \sin(\theta)}{\lambda} + \frac{2\pi n_{ox} f}{\lambda} - \frac{2\pi n_{ox}\sqrt{f^2 + x^2}}{\lambda} + 2m\pi \quad (2)$$

with $\lambda$ as the wavelength, $n_{ox}$ the refractive index of the oxide beneath the metal layer and $m$ an integer. $f$ is the focal distance, i.e., the distance at which all field components, originating from different parts of the lens, are in phase. This analytical phase delay can be mimicked by an array of slits with well-chosen widths [the red dots in Fig. 2(b)]. A closer look at Eq. (2) shows that the first term describes the prism action of the structure (tilting of the wave front), the second and third term introduce focusing (curvature of the wave front). The last term allows for the introduction of one or more $2\pi$ phase jumps in the phase front.

We validate the design with exact two-dimensional electromagnetic calculations based on a finite-difference frequency-domain (FDFD) method.[15] This method allows us to model materials using the measured, tabulated permittivity for every wavelength, thus directly taking into account both exact material dispersion as well as loss. The stated problem, however, requires the use of plane wave sources with varying angles of incidence, which cannot be realized with a finite line source.[16] We therefore implemented a modified version of the total-field/scattered-field method[16] for FDFD. In this method, the analytical field distribution that results from a plane wave interacting with a metal slab is used to generate the source term for the simulation of a metal slab with nanoscale slits, in contrast to the more generally used free-propagating plane wave. This way we can rigorously simulate, using a finite computational cell, the response of an isolated lens to an incident plane wave at an oblique angle of incidence. In all our simulations, we set the grid size to 2 nm in the transverse $x$ direction and 10 nm in the longitudinal $z$ direction.

The resulting magnetic field distribution (the real part of $H_y$) is shown in Fig. 2(c). Above the structure, the phase fronts make a 20° angle with the structure. Light couples to the slits, and as it propagates through the structure, the phase fronts experience the combination of tilt and curvature. As the light exits the structure, its phase front shows the curvature expected from a convex lens. The magnetic field intensity [Fig. 2(d)] confirms the focusing action of the lens. The focal length in FDFD is shorter than $f$, the analytical focal length from Eq. (2), because the lens' small dimensions limit the distance over which one can focus.[8,17] Because of the elongated focal spot, however, this should not pose a problem if a detector were placed at 4 $\mu$m distance from the lens structure. For this lens, the throughput ($z$-directed flux at the exit surface over $z$-directed flux over the width of the structure) is 58% and the efficiency ($z$-directed flux over the width of the photodiode over $z$-directed flux over the width of the structure) is 46%.

The presented design principles can be applied for light coming in under different angles, as shown in Fig. 3. All three lenses (for 10°, 30°, and 40°, which are realistic illumination angles for off-axis pixels in a solid-state image sensor) are designed with the same film thickness/slit length and can therefore, in practice, be patterned in the same set of processing steps. For the smallest angle, 10°, Fig. 3(a) shows that the required phase delay varies over less than $2\pi$. Therefore, we can reduce the metal spacing (to 20 nm) while keeping the same range of slit widths as in the structure in Fig. 2. Less spacing results in less phase delay introduced, better

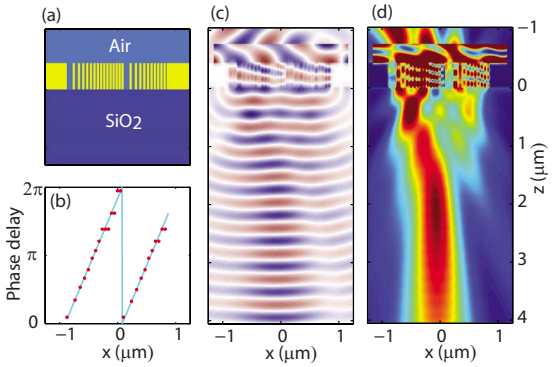


FIG. 4. (Color online) Nanoscale prism compensating for a 40° angle. (a) Geometry of the structure (same parameter space as Fig. 2). (b) The required phase delay (blue line), mimicked by the array of slits (red dots) (slit sequence: 100, 48, 34, 28, 24, 20, 18, 16, $3\times14$, $2\times12$, $2\times10$, 100, 50, 36, 28, 24, 20, 18, $2\times16$, and $2\times14$ nm). FDFD magnetic field (c) and magnetic field intensity pattern (d).

light in-coupling and less propagation loss. As a result, this lens has a higher throughput and efficiency (72% and 57%). The 30° and 40° designs require a full $2\pi$ (and more) phase delay [Figs. 3(b) and 3(c)]. They are designed with 40 nm metal spacing between slits. This results in throughputs/efficiencies that are slightly lower: 60%/46% (30°) and 59%/46% (40°). When comparing the focusing patterns of these lenses [Figs. 3(d)–3(f)], we see that they differ in the near-field, but are very similar in the far-field where it matters.

Figure 3(c) already indicates that tilting the wave front (the linear increase; prism action) dominates over the curvature introduced (focusing). It is instructive to look at a structure designed merely to tilt the wave front (i.e., a nanoscale patterned prism design). This also illustrates the effect of the aperture. Figure 4(b) shows the analytical phase delay and the delay introduced by the individual slits. The phase fronts in Fig. 4(c) are not curved like the ones in Fig. 2(c). The field intensity pattern in Fig. 4(d) still shows a focus, which is wider than the focal spots of the lenses from Figs. 2 and 3. As a result, less light ends up on a photodetector centered underneath the prism (throughput/efficiency: 60%/41%) and, for lens/prism arrays, there is more crosstalk.

Our first-principles simulation results confirm that the simplifying assumptions we made capture the main physics of the structures, namely that the lenses indeed focus right beneath the structures. The focal lengths, as observed in the exact numerical simulations, are quantitatively different from the analytical focal length. Several effects contribute to such discrepancy, the small size of the lens aperture being the main effect. Furthermore, in addition to the designed phase modulation, the structure modulates the amplitude of the light as well. Transmission cross sections vary for slits of different widths; certain slits are on/off resonance, resulting in high/low transmission locally. Propagation losses inside the slits depend on slit width as well. As an example, the symmetric mode of the narrowest slit (10 nm wide with 40 nm gold spacing) experiences a 35% loss over the thickness of the film. The phase delay of the light on exiting the structure is not exactly equal to what is analytically predicted [$\mathrm{Re}(\beta)d$]. A cavity effect, phase jumps upon entering and exiting the structure and interaction between nonidentical neighboring slits all influence the phase. These effects (that are not specifically designed for) have a much smaller influence on the efficiency of a structure than the main phase front design [from Eq. (2)]. They also indicate the fault tolerance of this approach and allow some more optimization.

The presented design principles are not limited to microlens design for solid-state image sensors. A wider range of optical and optoelectronic components could benefit from tailoring the phase front to redirect light.

The authors acknowledge Dr. Y. Ono and Dr. D. J. Tweet for helpful discussions. This research was supported by the Sharp Laboratories of America, the AFOSR-MURI program on plasmonics (Grant No. FA9550-1-0437), and the MARCO interconnect focus center.

[1] N. Engheta, Science **317**, 1698 (2007).
[2] V. M. Shalaev, Nat. Photonics **1**, 41 (2007).
[3] S. Lal, S. Link, and N. J. Halas, Nat. Photonics **1**, 641 (2007).
[4] Z. Sun and H. K. Kim, Appl. Phys. Lett. **85**, 642 (2004).
[5] H. Shi, C. Wang, C. Du, X. Luo, X. Dong, and H. Gao, Opt. Express **13**, 6815 (2005).
[6] T. Xu, C. Wang, C. Du, and X. Luo, Opt. Express **16**, 4753 (2008).
[7] Z. Sun, Appl. Phys. Lett. **89**, 261119 (2006).
[8] L. Verslegers, P. B. Catrysse, Z. Yu, J. S. White, E. S. Barnard, M. L. Brongersma, and S. Fan, Nano Lett. **9**, 235 (2009).
[9] Z. D. Popovic, R. A. Sprague, and G. A. Neville Connell, Appl. Opt. **27**, 1281 (1988).
[10] P. B. Catrysse and B. A. Wandell, Proc. SPIE **5678**, 1 (2005).
[11] K. Onozawa, K. Toshikiyo, T. Yogo, M. Ishii, K. Yamanaka, T. Matsuno, and D. Ueda, IEEE Trans. Electron Devices **55**, 986 (2008).
[12] *CRC Handbook of Chemistry and Physics*, 88th ed., edited by D. R. Lide (CRC, Boca Raton, 2007).
[13] E. N. Economou, Phys. Rev. **182**, 539 (1969).
[14] A. Yariv and P. Yeh, *Photonics: Optical Electronics in Modern Communications*, 6th ed. (Oxford University Press, New York, 2006).
[15] G. Veronis and S. Fan, in *Surface Plasmon Nanophotonics*, edited by M. L. Brongersma and P. G. Kik (Springer, New York, 2007), pp. 169–182.
[16] A. Taflove and S. Hagness, *Computational Electrodynamics: The Finite-Difference Time-Domain Method* (Artech House, Boston, 1995).
[17] P. Ruffieux, T. Scharf, H. P. Herzig, R. Völkel, and K. J. Weible, Opt. Express **14**, 4687 (2006).